Reconstructing Analytic Dinosaurs: Polynomial Eigenvalue Decomposition for Eigenvalues with Unmajorised Ground Truth

Sebastian J. Schlecht[1,2] and Stephan Weiss[3]
[1] *Acoustics Lab, Dept. of Information and Communications Engineering, Aalto University, Espoo, Finland*
[2] *Media Lab, Dept. of Art and Media, Aalto University, Espoo, Finland*
[3] *Dept. of Electronic & Electrical Eng., University of Strathclyde, Glasgow, Scotland*
sebastian.schlecht@aalto.fi, stephan.weiss@strath.ac.uk

***Abstract*—This paper proposes a novel method for accurately estimating the ground truth analytic eigenvalues from estimated space-time covariance matrices, where the estimation process obscures any intersection of eigenvalues with probability one. The approach involves grouping sufficiently separated, bin-wise eigenvalues into segments that belong to analytic functions and then solves a permutation problem to align these segments. By leveraging an inverse partial discrete Fourier transform and a linear assignment algorithm, the proposed *EigenBone* method retrieves analytic eigenvalues efficiently and accurately. Experimental results demonstrate the effectiveness of this approach in accurately reconstructing eigenvalues from noisy estimates. Overall, the proposed method offers a robust solution for approximating analytic eigenvalues in scenarios where state-of-the-art methods may fail.**

***Index Terms*—space-time covariance, eigenvalue decomposition, eigenvalue estimation, polynomial matrix.**

I. Introduction

Problems involving broadband multichannel data $\mathbf{x}[n] \in \mathbb{C}^M$ can be conveniently expressed via the space-time covariance $\mathbf{R}[\tau] = \mathcal{E}\{\mathbf{x}[n]\mathbf{x}^{\mathrm{H}}[n-\tau]\}$ where $\mathcal{E}\{\cdot\}$ is the expectation operator and $\{\cdot\}^{\mathrm{H}}$ the Hermitian transposition [1], [2]. The broadband equivalent to well-known narrowband solutions can then be reached via the diagonalisation of $\mathbf{R}[\tau]$ [3] for every lag $\tau \in \mathbb{Z}$ — or equivalently of its z-transform, the cross-spectral density (CSD) matrix $\boldsymbol{R}(z) = \sum_\tau \mathbf{R}[\tau] z^{-\tau}$ for every $z \in \mathbb{C}$ — by means of an eigenvalue decomposition (EVD) [3].

The EVD of a CSD matrix $\boldsymbol{R}(z) = \boldsymbol{Q}(z)\boldsymbol{\Lambda}(z)\boldsymbol{Q}^{\mathrm{P}}(z)$ exists with analytic factors, if $\mathbf{x}[n]$ is not associated with any multiplexing operations [4]–[6]. Then the paraunitary and diagonal matrix factors $\boldsymbol{Q}(z)$ and $\boldsymbol{\Lambda}(z)$ contain the analytic eigenvectors and the corresponding analytic eigenvalues, respectively. Paraunitarity implies that $\boldsymbol{Q}^{\mathrm{P}}(z) := \{\boldsymbol{Q}(1/z^*)\}^{\mathrm{H}} = \boldsymbol{Q}^{-1}(z)$, while the diagonal $\boldsymbol{\Lambda}(z)$ is parahermitian, such that $\boldsymbol{\Lambda}^{\mathrm{P}}(z) = \boldsymbol{\Lambda}(z)$. Analyticity is important, as it provides a low approximation order for polynomial (i.e. finite impulse response filter) approximations of $\boldsymbol{Q}(z)$ [7], [8]. This directly relates to the computational complexity and the latency of $\boldsymbol{Q}(z)$, which is important for applications such as the construction of paraunitary systems [9], [10], [12], [33] or polynomial subspace projections [13]–[16].

When working with an estimate $\hat{\mathbf{R}}[\tau]$ of the space-time covariance matrix, a fundamental challenge appears: independent of the sample size $N < \infty$ on which the estimate is based, the eigenvalues $\hat{\lambda}_m(z)$, $m = 1, \ldots, M$ will be spectrally majorised with probability one [17], i.e. on the unit circle we have that

$$\hat{\lambda}_m(\mathrm{e}^{\mathrm{j}\Omega}) > \hat{\lambda}_{m+1}(\mathrm{e}^{\mathrm{j}\Omega}), \ \ \forall \Omega \ \text{ and } \ m = 1, \ldots, (M-1), \ (1)$$

even if the eigenvalues in $\boldsymbol{\Lambda}(z)$ are unmajorised. Of the existing algorithms that target an EVD of $\hat{\boldsymbol{R}}(z)$, the approaches in [2], [18], [19] will favour (or can be shown to converge to [2]) spectral majorisation by design. More recent analytic extraction methods [7], [8], [20] will target the exact eigenvalues of $\hat{\boldsymbol{R}}(z)$ obeying (1). These algorithms will, therefore not find unmajorised eigenvalues of $\boldsymbol{R}(z)$, and at best converge to permuted, piecewise analytic functions as EVD factors, likely resulting in high approximation orders and perturbed subspaces.

Therefore, in this paper, we aim to define an algorithm capable to recovering functions close to the unmajorised eigenvalues of $\boldsymbol{R}(z)$ from an estimate $\hat{\boldsymbol{R}}(z)$. Our approach rests on a fundamental property of analytic functions; we recall this in the following theorem, whose unusual name is motivated by palaeontologists being seemingly able to reconstruct an entire dinosaur from some small bone fragment:

Theorem 1 (Dinosaur Bone Theorem): Given a small portion of an eigenvalue $\lambda(z)$ that is analytic in $z \in \mathbb{C}$, e.g. a segment on the unit circle, it is possible to reconstruct $\lambda(z)$ in its entirety.

Proof: Analytic functions are defined as matching their own Taylor series everywhere within their region of convergence. All derivatives required for the Taylor series expansion can therefore be determined from a non-vanishing, arbitrarily small segment, which we call here a *bone*. ■

In our approach, we find Q bones of eigenvalues $\hat{\boldsymbol{\Lambda}}(\mathrm{e}^{\mathrm{j}\Omega})$ within bands $\underline{\Omega}_q < \Omega < \overline{\Omega}_q$, $q = 1, \ldots, Q$ where the bin-wise eigenvalues are well separated and therefore are likely

S. Weiss' work was supported by the Engineering and Physical Sciences Research Council (EPSRC) Grant number EP/S000631/1 and the MOD University Defence Research Collaboration in Signal Processing.

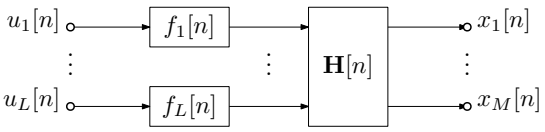

Fig. 1. Source model for measurement vector $\mathbf{x}[n]$.

to be spectrally majorised. For different bones from different frequency intervals, the Taylor series (i.e. time domain reconstruction) must be similar due to Theorem 1. Using a suitable clustering algorithm, we then line up bones to reconstruct an approximation of our dinosaur: the previously extinct, unmajorised eigenvalues of $\boldsymbol{R}(z)$. Thus, we name our approach the *EigenBone* Method.

Below, Sec. II outlines why estimated space-time covariance matrices possess spectrally majorised eigenvalues with probability one even if the ground truth eigenvalues are unmajorised, and motivates our proposed approach in Sec. III. Its results are characterised and benchmarked in Sec. IV. The Matlab code to reproduce all figures is provided online[1].

II. Problem Definition

A. Space-Time Covariance and Analytic EVD

Assume that the data vector $\mathbf{x}[n] \in \mathbb{C}^M$ emerges from the source model in Fig. 1. There, L mutually independent, temporally uncorrelated, zero mean, and unit variance Gaussian signals $u_\ell[n]$, $\ell = 1, \ldots, L$, excite innovation filters $f_\ell[n]$ that shape the sources' power spectral densities, prior to convolutive mixing by a system $\mathbf{H}[n] \in \mathbb{C}^{M \times L}$. Therefore, the cross-spectral density matrix $\boldsymbol{R}(z) \bullet\!\!-\!\!\circ\, \mathbf{R}[\tau]$ is given by

$$\boldsymbol{R}(z) = \boldsymbol{H}(z)\boldsymbol{F}(z)\boldsymbol{F}^{\mathrm{P}}(z)\boldsymbol{H}^{\mathrm{P}}(z)\ , \tag{2}$$

where $\boldsymbol{H}(z) \bullet\!\!-\!\!\circ\, \mathbf{H}[n]$ is a matrix of transfer functions of the mixing system, and $\boldsymbol{F}(z) = \mathrm{diag}\{f_1(z), \ldots, f_L(z)\}$ contains the L innovation filters $f_\ell(z) \bullet\!\!-\!\!\circ\, f_\ell[n]$ [21]. For causal and stable systems $\boldsymbol{F}(z)$ and $\boldsymbol{H}(z)$, $\boldsymbol{R}(z)$ in (2) is a matrix of functions that are guaranteed to be analytic on some annulus containing the unit circle [4]. Furthermore, because of the symmetries inherent in the auto- and cross-correlation sequences contained in $\mathbf{R}[\tau]$, the cross-spectral density is a parahermitian matrix i.e. $\boldsymbol{R}(z) = \boldsymbol{R}^{\mathrm{P}}(z)$.

For analytic parahermitian matrices that are derived from unmultiplexed signals $\mathbf{x}[n]$, there exists an EVD with analytic factors [5], [6],

$$\boldsymbol{R}(z) = \boldsymbol{Q}(z)\boldsymbol{\Lambda}(z)\boldsymbol{Q}^{\mathrm{P}}(z)\ . \tag{3}$$

The diagonal matrix $\boldsymbol{\Lambda}(z) = \mathrm{diag}\{\lambda_1(z), \ldots, \lambda_M(z)\}$ contains the analytic eigenvalues. Their corresponding analytic eigenvectors form the columns of the paraunitary matrix $\boldsymbol{Q}(z)$, such that $\boldsymbol{Q}^{-1}(z) = \boldsymbol{Q}^{\mathrm{P}}(z)$. If in the source model of Fig. 1 the mixing matrix $\boldsymbol{H}(z)$ is paraunitary, then we have $\boldsymbol{Q}(z) = \boldsymbol{H}(z)$ and $\boldsymbol{\Lambda}(z) = \boldsymbol{F}(z)\boldsymbol{F}^{\mathrm{P}}(z)$. The analyticity of the EVD factors has two important implications: (i) functions are unique within their region of convergence [22], and (ii) while the factors may represent infinite series, they can be arbitrarily close approximated by polynomials of sufficiently high order through shift and truncation operations [7], [8].

[1] https://github.com/SebastianJiroSchlecht/EigenBones

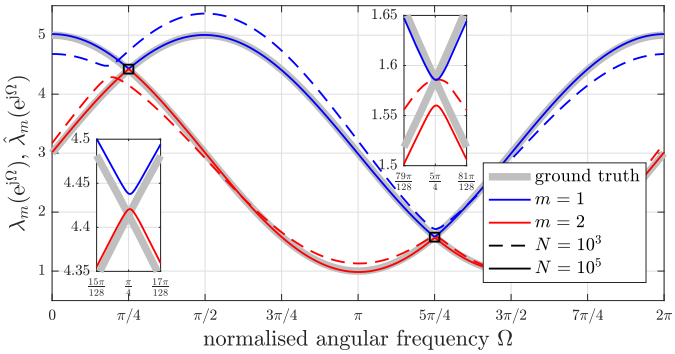

Fig. 2. Example of analytic eigenvalues of $\boldsymbol{R}(z)$ ($N \to \infty$) and of its estimate $\hat{\boldsymbol{R}}(z)$ for samples sizes $N \in \{10^3, 10^5\}$.

B. Impact of Space-Time Covariance Estimation

If space-time covariance matrices are estimated from data $\mathbf{x}[n]$, $0 \leqslant n < N$ via their best linear unbiased estimator, then the variance of the estimate $\hat{\mathbf{R}}[\tau]$ with respect to the ground truth $\mathbf{R}[\tau]$ given by the source model in Fig. 1 depends on both the sample size N and on $\mathbf{R}[\tau]$ [23]. This estimation error leads to a perturbation of both the eigenvalues and eigenspaces [24]. On the unit circle and in a bin-wise view, this perturbation tends to reduce as N increases [25], and one might be misled to think that the analytic EVD of $\hat{\boldsymbol{R}}(\mathrm{e}^{\mathrm{j}\Omega}) = \hat{\boldsymbol{Q}}(\mathrm{e}^{\mathrm{j}\Omega})\hat{\boldsymbol{\Lambda}}(\mathrm{e}^{\mathrm{j}\Omega})\hat{\boldsymbol{Q}}^{\mathrm{P}}(\mathrm{e}^{\mathrm{j}\Omega})$ converges towards that of $\boldsymbol{R}(z)|_{z=\mathrm{e}^{\mathrm{j}\Omega}}$ in (3).

If on the unit circle the eigenvalues of $\boldsymbol{\Lambda}(\mathrm{e}^{\mathrm{j}\Omega})$ intersect, they must possess an algebraic multiplicity greater than one for some Ω. In contrast, since the eigenvalues of $\hat{\boldsymbol{\Lambda}}(\mathrm{e}^{\mathrm{j}\Omega})$ are drawn from a distribution, they will be distinct with probability one [26], which applies for every frequency Ω. As a result, the eigenvalues of $\hat{\boldsymbol{\Lambda}}(\mathrm{e}^{\mathrm{j}\Omega})$ will no longer intersect, and be spectrally majorised with probability one [17].

Example 1: Consider data generated according to Fig. 1 with $f_1(z) = (1 + az^{-1})/\sqrt{a}$ with $a = \frac{1}{2}(3 - \sqrt{5})$, $f_2(z) = (1 + \mathrm{j}az^{-1})/\sqrt{a}$ and a paraunitary $\boldsymbol{H}(z) = [1,\ 1;\ z^{-1},\ -z^{-1}]$, which yields the CSD matrix

$$\boldsymbol{R}(z) = \begin{bmatrix} \frac{1-\mathrm{j}}{2}z + 3 + \frac{1+\mathrm{j}}{2}z^{-1} & \frac{1+\mathrm{j}}{2}z^{2} + \frac{1-\mathrm{j}}{2} \\ \frac{1+\mathrm{j}}{2} + \frac{1-\mathrm{j}}{2}z^{-2} & \frac{1-\mathrm{j}}{2}z + 3 + \frac{1+\mathrm{j}}{2}z^{-1} \end{bmatrix} \tag{4}$$

taken from [3]. The eigenvalues of $\boldsymbol{R}(z)$ are the source power spectral densities, i.e. $\lambda_m(z) = f_m(z)f^{\mathrm{P}}{}_m(z)$, $m = 1, 2$, as shown in Fig. 2, with $\lambda_1(\mathrm{e}^{\mathrm{j}\Omega}) = 3 + 2\cos\Omega$ and $\lambda_2(\mathrm{e}^{\mathrm{j}\Omega}) = 3 + 2\sin\Omega$. For estimates $\hat{\boldsymbol{R}}(z)$ based on sample sizes of $N = 10^3$ and $N = 10^5$, Fig. 2 shows the analytic eigenvalues $\hat{\lambda}_m(\mathrm{e}^{\mathrm{j}\Omega})$, which are now spectrally majorised. The non-trivial algebraic multiplicities of $\boldsymbol{\Lambda}(\mathrm{e}^{\mathrm{j}\Omega})$ at $\Omega_1 = \frac{\pi}{4}$ and $\Omega_2 = \frac{5\pi}{4}$ have disappeared, and $\hat{\boldsymbol{\Lambda}}(\mathrm{e}^{\mathrm{j}\Omega})$ is made up of piecewise analytic bones that are permuted at Ω_i, $i = 1, 2$. △

The above Example 1 has highlighted that while the per-bin or per-frequency estimation error reduces, the eigenvalues of the estimated space-time covariance matrices remain spectrally majorised even for very large sample sizes N. This has two profound consequences: (i) we are unable to obtain the ground truth eigenvalues if we adhere strictly to $\hat{\boldsymbol{R}}(z)$ for any realistic sample size N; (ii) even if the ground truth has compact support, by increasing the sample size N, the approximation order increases dramatically with N, since the analytic EVD factors of $\hat{\boldsymbol{R}}(z)$ converge towards piecewise analytic functions. If the ground truth eigenvalues are unmajorised, then the target eigenvalues $\hat{\boldsymbol{\Lambda}}(\mathrm{e}^{\mathrm{j}\Omega})$ will aim to approximate non-differentiable functions, and the eigenvectors in $\hat{\boldsymbol{Q}}(z)$ will converge towards discontinuities. This leads to high approximation orders and to significant perturbation of the associated the eigenspaces close to non-trivial algebraic multiplicities of $\boldsymbol{\Lambda}(\mathrm{e}^{\mathrm{j}\Omega})$.

III. Proposed EigenBone Method

The proposed method aims to retrieve the ground truth eigenvalues from an estimated space-time covariance matrix $\hat{\boldsymbol{R}}(z)$ via a bin-wise EVD $\hat{\boldsymbol{R}}(\mathrm{e}^{\mathrm{j}\Omega_k}) = \hat{\mathbf{Q}}_k \hat{\boldsymbol{\Lambda}}_k \hat{\mathbf{Q}}_k^{\mathrm{H}}$, with $\Omega_k = \frac{2\pi k}{K}$, $k = 0, \ldots, (K-1)$, for a K-point discrete Fourier transform (DFT). The eigenvalues in $\hat{\boldsymbol{\Lambda}}_k = \mathrm{diag}\{\hat{\lambda}_{1,k}, \ldots, \hat{\lambda}_{M,k}\}$ are assumed to be majorised.

A. Determining Analytic Bones

The first step involves determining the analytic bones. A bone is defined as a succession of bins with a sufficient eigenvalue separation. In the kth bin, we measure this separation as the minimum distance, $\delta_k = \min_m(\hat{\lambda}_{m,k} - \hat{\lambda}_{m+1,k})$ between any two eigenvalues, and define a threshold $\mathcal{T}$ above which we treat eigenvalues as sufficiently far apart such that an intersection of the ground truth eigenvalues is unlikely. Let Q be the number of bones that we can identify. Each bone's bounds, $\underline{\Omega}_q$ and $\overline{\Omega}_q$, can be determined by maximizing the frequency range while ensuring a sufficient separation δ_k between adjacent eigenvalues, i.e.

$$\max_{\underline{\Omega}_q, \overline{\Omega}_q} (\overline{\Omega}_q - \underline{\Omega}_q) \quad \text{s.t.} \quad \delta_k > \mathcal{T}\,, \forall \Omega_k \in [\underline{\Omega}_q,\, \overline{\Omega}_q]\,. \tag{5}$$

In order to be workable, as the Q bones we only retain those that satisfy a minimum length across successive bins, i.e. $(\overline{\Omega}_q - \underline{\Omega}_q) > \mathcal{B}$ for some threshold $\mathcal{B}$.

Example 2: To demonstrate the segmentation approach for the estimated space-time covariance $\hat{\boldsymbol{R}}[\tau]|_{N=10^3}$ of Example 1, Fig. 3 shows the minimum eigenvalue distance per bin for a 2^{10}-point DFT, a threshold $\mathcal{T} = \frac{1}{16}$, and the resulting $Q = 2$ bones, of which the first is wrapped. △

Determining the appropriate threshold $\mathcal{T}$ for segmentation can be challenging due to the trade-off between bone accuracy and computational feasibility. If the threshold is too high, numerous bones are detected, rendering the subsequent assignment problem ill-conditioned. Conversely, setting the threshold too low may result in missed eigenvalue intersections, leading to inaccuracies in recovering the ground truth eigenvalues.

In practice, missing an intersection tends to be more detrimental than splitting bones into smaller portions, as it can

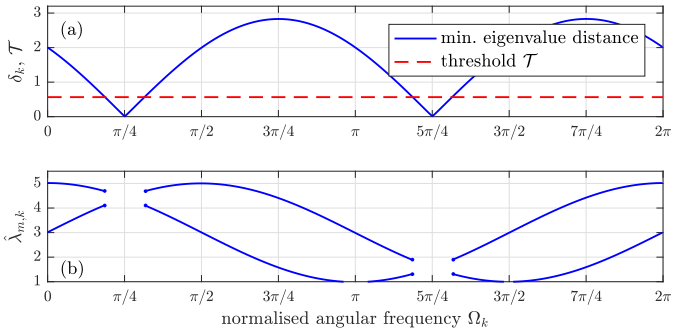

Fig. 3. (a) Minimum eigenvalue distance δ_k and threshold $\mathcal{T}$, and (b) the resulting $Q = 2$ bones for the matrix $\hat{\mathbf{R}}[\tau]$ from Example 1.

significantly affect the accuracy of the reconstructed eigenvalues. To address this, more sophisticated splitting criteria can be devised. For example, utilizing higher-order derivatives or considering additional spectral characteristics may provide a more robust bone division, enhancing the accuracy of eigenvalue retrieval. For more complex scenarios with a larger number of eigenvalues, it may also be advisable to split each eigenvalue independently into bones.

B. Solving the Permutation Problem

To associate the eigenvalue bones, we project each of the bones onto a common basis using an inverse partial discrete Fourier transform (iDFT), facilitating the recovery of time-domain coefficients for each bone. The linear least-squares problem

$$\ell_{m,q}[\tau] = \underset{\ell[\tau]}{\mathrm{argmin}} \sum_{\Omega_k \in \mathcal{W}_q} \left| \sum_{\tau \in S} \ell[\tau] \mathrm{e}^{-\mathrm{j}\Omega_k \tau} - \hat{\lambda}_{m,k} \right|^2, \tag{6}$$

with $\mathcal{W}_q = \{\underline{\Omega}_q, \ldots, \overline{\Omega}_q\}$, aims to determine the time-domain coefficients $\ell_{m,q}[\tau]$ of the q^{th} bone of the m^{th} eigenvalue. In (6), $S = \{-s, \ldots, -1, 0, 1, \ldots, s\}$ denotes the support of the time-domain coefficients. Since the ill-conditioning of the least squares problem (6) increases with shorter bones $(\overline{\Omega}_q - \underline{\Omega}_q)$ and larger temporal supports S, we generally select $S \ll \mathcal{B}$. Sophisticated methods for signal extrapolation within limited bandwidths, such as the Papoulis-Gerchberg algorithm and its extensions, can also help to address this issue [27]–[29].

Example 3: For bones in Fig. 3 as part of Example 2, Fig. 4 illustrates the reconstructions via (6) with a maximum lag $s = 2$. On this reconstructed common basis, it is easy to associate the matching functions: With respect to the first bone in the l.h.s. plots, the eigenvalues in the second bone in the r.h.s. plots are swapped. △

The permutation problem is then formulated as a linear assignment problem, with the Hungarian algorithm [30] being one efficient method for its solution. This algorithm minimizes the cost of associating bones, as expressed by:

$$\min_{\mathbf{P}} \mathrm{tr}\{\mathbf{CP}\}\,, \tag{7}$$

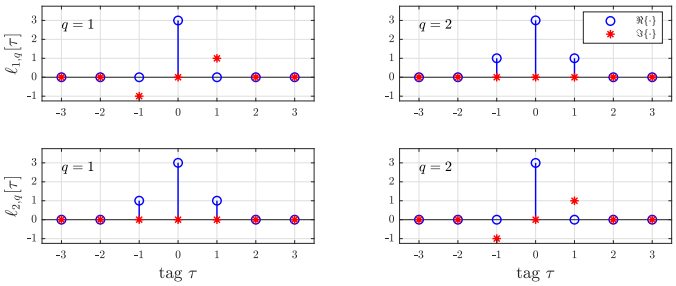

Fig. 4. Time domain functions derived from the $Q = 2$ bones via (6).

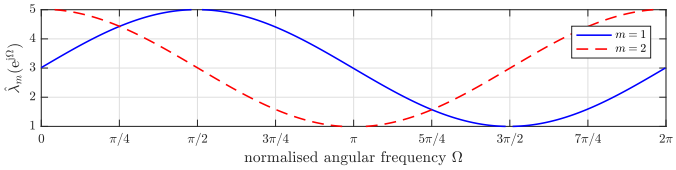

Fig. 5. Retrieved analytic eigenvalues based on the proposed method for Example 1.

where $\mathbf{P}$ is a permutation matrix and $\mathbf{C} \in \mathbb{R}^{M\times M}$ is the cost matrix defined as:

$$C_{ij} = \sum_{\tau\in S} |\ell_{i,1}[\tau] - \ell_{j,q}[\tau]|^2 \quad \text{for } 1 \leqslant i,j \leqslant M \ . \tag{8}$$

Here, the first bone is arbitrarily chosen as the reference. Instead of matching every bone with the first bone iteratively, a multi-way matching approach can be employed [31]. Solving the assignment problem (7) for each q yields the index permutation $p_q(m)$, aligning the bones $\ell_{m,1}, \ell_{p_2(m),2}, \ldots, \ell_{p_Q(m),Q}$ to form the m^{th} aligned eigenvalue.

C. Eigenvalue Retrieval

Once the permutations are resolved, the eigenvalues can be determined using various methods. A simple approach involves bone-size weighted averaging, such that for the approximated analytic eigenvalues $\hat{\lambda}_m[\tau]$, we have that

$$\hat{\lambda}_m[\tau] = \frac{1}{\sum_q |\mathcal{W}_q|} \sum_{q=1}^{Q} |\mathcal{W}_q| \cdot \ell_{m,q}[\tau] \ , \tag{9}$$

with $|\mathcal{W}_q|$ the number of bins in the q^{th} bone. Such a time-domain averaging approach takes into account that longer bones tend to provide more accurate results and offers the advantage of statistical averaging across the entire frequency range. Ultimately, the discrete Fourier transform of $\hat{\lambda}_m[\tau]$ yields the reconstructed unmajorized frequency-domain eigenvalues $\hat{\lambda}_m(\mathrm{e}^{\mathrm{j}\Omega})$.

Example 4: The reconstruction of the above example based on the time domain bone functions $\ell_{m,q}[\tau]$ in Fig. 4 via (9) is shown Fig. 5. The retrieved eigenvalues accurately match the unmajorised ground truth in Fig. 2. △

IV. Results

We demonstrate the proposed method's effectiveness in one comparative example as well as in one challenging scenario.

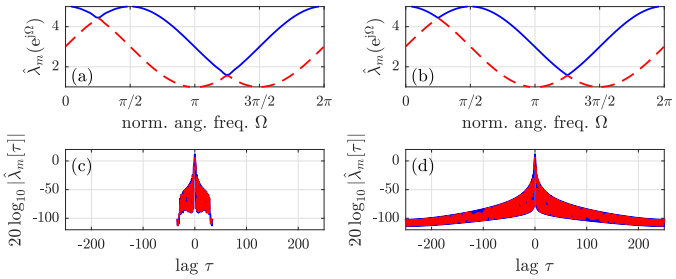

Fig. 6. Benchmark methods applied to $\hat{\boldsymbol{R}}(z)|_{N=10^5}$ with approximated eigenvalues $\hat{\lambda}_m(\mathrm{e}^{\mathrm{j}\Omega})$ for (a) SMD [19] and b) [7], and the decay of their time domain coefficients for (c) SMD and (d) [7].

A. Comparison to State-of-the-Art

Examples 2-4 have explored the application of the proposed approach to the system in Example 1 with $N = 10^5$ samples. The resulting approximated eigenvalues in Fig. 5 closely matched the unmajorised ground truth functions. In contrast, applying the polynomial EVD algorithms such as sequential matrix diagonalisation (SMD) algorithm (with a maximum of 200 iterations, [19]) and the analytic eigenvalue extraction method in [7] to the same parahermitian matrix yields the estimates shown in Fig. 6. SMD is known to yield only incomplete diagonalisation [4], and neither algorithm can recover the unmajorised ground truth. Additionally, since in particular [7] tries to closely approximate functions that are only piecewise analytic, the decay of the eigenvalue coefficients as shown in Fig. 6(d) is poor. By comparison, the proposed method yields a finite time domain support of only seven coefficients for the results in Fig. 5.

B. Challenging Scenario

For a more challenging scenario (Example 4 in [8]), the $M = 3$ ground truth eigenvalues $\lambda_m(\mathrm{e}^{\mathrm{j}\Omega})$ are given in Fig. 7(a), together with their bin-wise estimates based on $N = 10^5$ samples. With $K = 2^{10}$ bins and a threshold $\mathcal{T} = \frac{1}{8}$ according to (5) for the minimum eigenvalue distance, the proposed method yields the segmentation in Fig. 7(b). There are now $Q = 5$ bones of various lengths, and intervals where at least some of the eigenvalues are closely spaced have been excluded. The reconstructions of the individual bones via (6) yield the time domain functions in Fig. 8, and it is a straightforward process to associate functions across the $Q = 5$ different bones. The bone-size weighted reconstruction from the time-domain bones using (9) yields the approximations in Fig. 9. Our method retrieves eigenvalues close to the ground truth, even accurately reconstructing the middle section near $\Omega = \pi$ that was initially discarded in the segmentation process.

V. Conclusion

We have presented a novel method for accurately recovering unmajorized eigenvalues from space-time covariance matrices, where the estimation from data will obscure the analytic eigenvalues with probability one. Our approach demonstrates

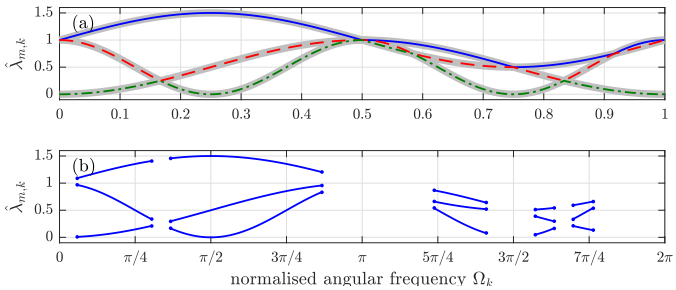

Fig. 7. (a) Spectrally majorised association of bin-wise eigenvalues with ground truth underlaid in grey; (b) segmentation result.

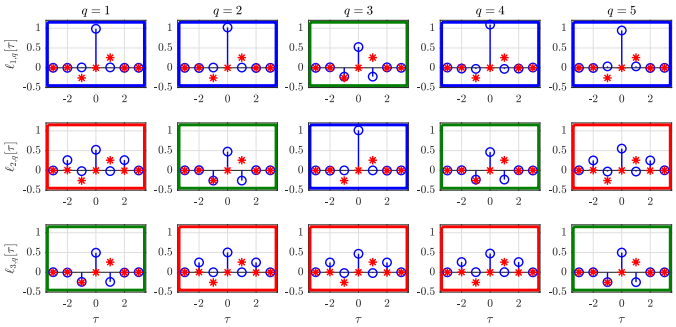

Fig. 8. Time domain functions $\ell_{m,q}[\tau]$ reconstructed from bones with real (○) and imaginary parts (∗). The axis position indicates the majorised order of bones, while the frame color shows the resolved permutation.

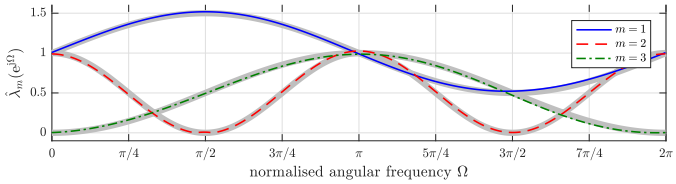

Fig. 9. Retrieved unmajorised analytic eigenvalues.

robustness in handling noisy data and complex scenarios, as illustrated through two examples. By leveraging segmentation and time-domain coefficient matching, our method achieves superior performance compared to the state-of-the-art, both in terms of retrieving the analytic unmajoried eigenvalues as well as achieving a low order approximation. These results show the potential of our method to uncover correct spectral associations in broadband array processing, with important applications, e.g., for finite data subspace methods [13]–[16] and extentions to the analytic SVD [32] and its applications [33].

References

[1] P.P. Vaidyanathan, *Multirate Systems and Filter Banks*. Englewood Cliffs: Prentice Hall, 1993.

[2] J.G. McWhirter, P.D. Baxter, T. Cooper, S. Redif, and J. Foster, "An EVD Algorithm for Para-Hermitian Polynomial Matrices," *IEEE Trans. SP*, **55**(5):2158–2169, May 2007.

[3] V. Neo, S. Redif, J. McWhirter, J. Pestana, I. Proudler, S. Weiss, and P. Naylor, "Polynomial eigenvalue decomposition for multichannel broadband signal processing," *IEEE SP Mag.*, **40**(7):18–37, Nov. 2023.

[4] S. Weiss, J. Pestana, and I.K. Proudler, "On the existence and uniqueness of the eigenvalue decomposition of a parahermitian matrix," *IEEE Trans. SP*, **66**(10):2659–2672, May 2018.

[5] S. Weiss, J. Pestana, I.K. Proudler, and F.K. Coutts, "Corrections to "On the existence and uniqueness of the eigenvalue decomposition of a parahermitian matrix"," *IEEE Trans. SP*, **66**(23):6325–6327, Dec. 2018.

[6] G. Barbarino and V. Noferini, "On the Rellich eigendecomposition of para-Hermitian matrices and the sign characteristics of ∗-palindromic matrix polynomials," *Linear Algebra Appl.*, **672**:1–27, Sep. 2023.

[7] S. Weiss, I. K. Proudler, and F. K. Coutts, "Eigenvalue decomposition of a parahermitian matrix: extraction of analytic eigenvalues," *IEEE Trans. SP*, bf 69:722–737, Jan. 2021.

[8] S. Weiss, I. Proudler, F. Coutts, and F. Khattak, "Eigenvalue decomposition of a parahermitian matrix: extraction of analytic eigenvectors," *IEEE Trans. SP*, bf 71:1642–1656, Apr. 2023.

[9] S.J. Schlecht and E.A.P. Habets, "On Lossless Feedback Delay Networks," *IEEE Trans. SP*, **65**(6):1554 – 1564, 2017.

[10] S.J. Schlecht, "Allpass feedback delay networks," *IEEE Trans. SP*, **69**:1028–1038, 2021.

[11] S. Weiss, S.J. Schlecht, O. Das, and E. De Sena, "Polynomial Procrustes problem: Parаunitary approximation of matrices of analytic functions," in *EUSIPCO*, Helsinki, Finland, 2023.

[12] O. Das, S.J. Schlecht, and E. De Sena, "Grouped feedback delay networks with frequency-dependent coupling," *IEEE/ACM Trans. ASLP*, **31**:2004–2015, May 2023.

[13] S. Weiss, S. Bendoukha, A. Alzin, F. Coutts, I. Proudler, and J. Chambers, "MVDR broadband beamforming using polynomial matrix techniques," in *EUSIPCO*, Nice, France, Sep. 2015, pp. 839–843.

[14] S. Weiss, C. Delaosa, J. Matthews, I. Proudler, and B. Jackson, "Detection of weak transient signals using a broadband subspace approach," in *SSPD*, Edinburgh, Scotland, Sep. 2021, pp. 65–69.

[15] C.A.D. Pahalson, L.H. Crockett, and S. Weiss, "Detection of Weak Transient Broadband Signals Using a Polynomial Subspace and Likelihood Ratio Test Approach", in *EUSIPCO*, Lyon, France, Aug. 2024.

[16] V. Neo, C. Evers, S. Weiss, and P. Naylor, "Signal compaction using polynomial EVD for spherical array processing with applications," *IEEE/ACM Trans. ASLP*, **31**:3537–3549, 2023.

[17] F.A. Khattak, S. Weiss, I.K. Proudler, and J.G. McWhirter, "Space-time covariance matrix estimation: Loss of algebraic multiplicities of eigenvalues," in *Asilomar SSC*, Pacific Grove, CA, Oct. 2022.

[18] S. Redif, J. McWhirter, and S. Weiss, "Design of FIR paraunitary filter banks for subband coding using a polynomial eigenvalue decomposition," *IEEE Trans. SP*, **59**(11):5253–5264, Nov. 2011.

[19] S. Redif, S. Weiss, and J. McWhirter, "Sequential matrix diagonalization algorithms for polynomial EVD of parahermitian matrices," *IEEE Trans. SP*, **63**(1):81–89, Jan. 2015.

[20] M. Tohidian, H. Amindavar, and A. M. Reza, "A DFT-based approximate eigenvalue and singular value decomposition of polynomial matrices," *EURASIP JASP*, **2013**(1):1–16, 2013.

[21] A. Papoulis, *Probability, Random Variables, and Stochastic Processes*, 3rd ed. New York: McGraw-Hill, 1991.

[22] L. V. Ahlfors, *Complex analysis: An introduction to the theory of analytic functions of one complex variable*. NY: McGraw-Hill, 1953.

[23] C. Delaosa, J. Pestana, N. J. Goddard, S. Somasundaram, and S. Weiss, "Sample space-time covariance matrix estimation," in *IEEE ICASSP*, Brighton, UK, May 2019, pp. 8033–8037.

[24] T. Kato, *Perturbation Theory for Linear Operators*. Springer, 1980.

[25] C. Delaosa, F. K. Coutts, J. Pestana, and S. Weiss, "Impact of space-time covariance estimation errors on a parahermitian matrix EVD," in *IEEE SAM*, July 2018, pp. 1–5.

[26] X. Mestre, "On the asymptotic behavior of the sample estimates of eigenvalues and eigenvectors of covariance matrices," *IEEE Trans. SP*, **56**(11):5353–5368, Nov. 2008.

[27] P. Ferreira, "Interpolation and the discrete Papoulis-Gerchberg algorithm," *IEEE Trans. SP*, **42**(10):2596–2606, 1994.

[28] M. Marques, A. Neves, J.S. Marques, and J. Sanches, "The Papoulis-Gerchberg Algorithm with Unknown Signal Bandwidth," ser. Lecture Notes in Computer Science, 2006, pp. 436–445.

[29] B.G. Salomon and H. Ur, "A Method for the Recovery of Gaps in General Analytic Signals," *ISRN Signal Proc.*, **2011**:1–6, 2011.

[30] H.W. Kuhn, "The Hungarian method for the assignment problem," *Naval Research Logistics Quarterly*, **2**(1-2):83–97, 1955.

[31] D. Pachauri, R. Kondor, and V. Singh, "Solving the multi-way matching problem by permutation synchronization," in *Advances in Neural Information Processing Systems*, **26**, Curran Associates, Inc., 2013.

[32] S. Weiss, I.K. Proudler, G. Barbarino, J. Pestana, and J. G. McWhirter, "On properties and structure of the analytic singular value decomposition," *IEEE Trans. SP*, **72**:2260–2275, Apr. 2024.

[33] S. Weiss, S.J. Schlecht, O. Das, and E. De Sena, "Polynomial Procrustes Problem: Parаunitary Approximation of Matrices of Analytic Functions", in *EUSIPCO*, Helsinki, Finland, Sep. 2023.